# Influence of internal interfacial area on nanosecond relaxation of wheat gluten proteins as probed by broadband ultrasonic spectroscopy

Y. Fan [a], M.G. Scanlon [b,*], J.H. Page [a]

[a] Department of Physics & Astronomy, University of Manitoba, Winnipeg, Manitoba, Canada R3T 2N2
[b] Department of Food Science, University of Manitoba, Winnipeg, Manitoba, Canada R3T 2N2

**ABSTRACT**

Understanding interactions between interfaces and biopolymers in complex industrially processed materials of plant origin will allow for their better utilization. Wheat flour doughs are one such material whose industrial use strongly depends on such interactions due to their effect on the mechanical properties of the dough. To date, mechanical characterizations of dough have been limited to a narrow range of frequencies. Here, ultrasonic spectroscopy measurements over a very broad frequency range are used to show that a fast volumetric relaxation occurs in dough; the nanosecond timescale of the relaxation is associated with ultrasonic stress-induced changes in the secondary structure of gluten proteins. Interestingly, there is a four-fold difference in the speed of this relaxation phenomenon in doughs mixed in air (where substantial internal interfacial area exists) compared to those mixed under vacuum (where bubbles are absent). Given the large internal interfacial area in dough, the amphiphilic proteins residing at gas bubble interfaces significantly alter the high-frequency mechanical response of this important material.

## 1. Introduction

The complex mixture of structured biopolymers extracted from wheat endosperm is one of our planet's great renewable resources [1,2]. Understanding the structure, properties and dynamics of the hydrated version of this resource is essential for more efficient conventional use of the material in a variety of foods [2–4], but also for its better exploitation in the manufacture of industrial products [2,5–7].

During conventional processing, the dough that is formed from refined wheat endosperm particles occludes a significant volume fraction of air [8–11]; its value varies with the gas pressure exerted on the dough surface [9,12], the viscosity of the dough [13–15], and the type and duration of the process [10,11]. In emphasizing the importance to end-product characteristics of gas entrapment by the viscoelastic network, it has been stated that "gas production and retention are the keys to breadmaking" [16]. Further evidence of the significance of gas-holding to end-use properties is the utilization of cutting-edge techniques, such as the European Synchrotron Radiation Facility, to understand gas-holding functionality [17–19].

As well as influencing end-product properties, the gas content and how the gas is distributed within the dough affect its physical properties [20–22]. A typical median diameter of air bubbles that is nucleated in a breadmaking dough is 100 μm [23–25], so that with dough's typical volume fraction of air of 0.1, dough has a substantial internal interfacial area. An interfacial area to volume ratio of $1400\,m^{-1}$ is a typical figure for dough [26], a value that is not dissimilar to classically porous materials such as bone [27,28] and some porous ceramics [29]. In a theoretical examination of the influence of internal interfacial area on the mechanical properties of dough, it was concluded that 80% of the strain energy in a dough deformed to 4% strain arose from changes in dough's interfacial free energy [26].

An additional consequence of a large internal interfacial area is that the interface is a preferential location for the many of the surface-active biopolymers that are present in dough [30–32]. Such molecules have been assigned significant roles in the end-use performance of products made from dough [31,33,34], but few studies have investigated the mechanical significance of these surface-active molecules. This contrasts with highly aerated food systems, where numerous studies examining the link between the mechanical properties (rheology) of foams and the type of surface-active biopolymer [35–37], its conformation at the interface [35,38,39], or its dynamics [36,40] have been conducted. In such investigations, spectroscopic techniques are intensively used tools;

* Corresponding author. Tel.: +1 2044746480.
 E-mail address: scanlon@cc.umanitoba.ca (M.G. Scanlon).

pertinent examples are circular dichroism, Raman optical activity and polarization-modulation infrared reflection–absorption spectroscopy being used to probe the secondary structures of protein at an interface [35,38], the conformational stability of wheat proteins [41] and the synergy in the interfacial adsorption between surface-active proteins [42], respectively.

In addition to being effective at probing the effect of gas bubbles on the mechanical properties of biological materials [12,22], ultrasound has a long history as a spectroscopic technique for determining the mechanical response of polymer molecules at high frequencies [43]. By utilizing ultrasound over a wide range of frequencies, a variety of interesting phenomena that operate at different time scales can be interrogated. Given the broad distribution of relaxation times that is evident in dough [44–46], the insights from high frequency assessments of mechanical behavior allow a fuller characterization of dough's mechanical response and how this response is affected by the internal interfaces in the dough. However, to date there have been few high frequency investigations of dough properties, in large part because the highly absorptive nature of wheat flour dough makes accurate measurements of ultrasonic velocity and attenuation experimentally challenging [22,47]. In particular, determining the mechanical response of dough's hydrated viscoelastic network is hindered by strong ultrasonic absorption associated with the broad resonance peak arising from the polydisperse distribution of bubbles that is present in the dough [22,48].

The purpose of this paper is to report on ultrasonic spectroscopy measurements of wheat flour dough (made without yeast) using longitudinally polarized pulses over a wide frequency range (50 kHz to 30 MHz, by far the broadest frequency range yet reported). To ascertain how the large interfacial area associated with the gas bubbles in dough affects its mechanical response, dough was also mixed under vacuum to provide a reference material in which the internal interfacial area associated with these bubbles is minimized.

## 2. Experimental

### 2.1. Materials

Doughs were prepared from 100 g of a strong breadmaking flour (CWRS) that had been milled on the CIGI pilot mill (Winnipeg, MB, Canada). Reagent grade (Fisher Scientific, Nepean, ON, Canada) sodium chloride (2.4 g) was dissolved in 61 ml of distilled water that was then mixed with the flour. A high-speed pin-mixer, specifically a GRL-200 recording mixer [49], operating at 225 rpm, was used to mechanically develop the dough's viscoelastic network. Doughs were mixed for 5.5 min, the optimal mixing time as assessed from a torque vs mixing time curve when dough was prepared at atmospheric pressure.

To mix doughs under vacuum, the GRL-200 mixer was coupled to a vacuum pump via a digital pressure gauge and control valve to record and control headspace pressure during mixing. Vacuum grease was used to seal the mixing bowl. Ingredients were identical to those of the dough mixed at atmospheric pressure, but they were mixed for 1 min before evacuation to allow the flour to hydrate so that flour particles would not be drawn out. Vacuum mixing was therefore conducted for the last 4.5 min of mixing for a total time of 5.5 min.

After mixing, the dough piece was stored in a sealed container. Subsamples were cut from the dough piece with scissors; size was chosen according to the thickness to which the subsample was to be compressed. Subsample mass was determined from the difference of the mass of the container with the dough piece before and after excising the subsample.

Subsamples were also removed to determine dough density by weight in air and weight in water measurements [11,12].

### 2.2. Ultrasonic measurements

Two sets of apparatus were used for ultrasonic transmission measurements: one for low and very high frequency measurements (40 kHz, 20 MHz), and the other for high frequency measurements (500 kHz and greater). Block diagrams are shown in Fig. 1, with all connections made with 50 Ω BNC cables. Pairs of ultrasonic transducers were purchased from Panametrics (Olympus NDT, Waltham, MA).

In the low-frequency set-up, transducers were nominally 50 kHz, but their central frequency was ascertained as approximately 40 kHz. In the high frequency experiments, various transducer pairs of different central frequencies were employed (1.0, 2.25, 5.0 and 20 MHz). Two sets of transducer holders were used to contain the dough subsamples: direct contact and acrylic plate delay measurements. Direct contact between dough and transducers was used for the majority of measurements.

In the contact measurement holder, three micrometers, with a range of 28 mm, dictated the separation of the two steel plates (and thus the separation between the transducers). The dough subsample was compressed to the desired separation by manipulating the three micrometers. Securing screws were then set to maintain plate separation and hence sample thickness (Fig. 1a).

The acrylic plate delay measurement holder was used for the higher frequency measurements of doughs that had been mixed at atmospheric pressure (500 kHz to 5 MHz, but not the 20 MHz measurements). Copper plates (each 0.30 mm thick) were inserted between the acrylic plates to control dough subsample thickness. Two transducers, secured by clamps that allowed transducer alignment to be adjusted, were bonded via coupling gel to the acrylic plates (Fig. 1b).

In order to make the area covered by the compressed subsample essentially identical at different thicknesses, the mass of the subsample was selected for the low frequency measurements by:

$$m = \pi R^2 d\rho, \tag{1}$$

where $R$ is the desired radius of coverage, $d$ is the thickness of the subsample that was analyzed, and $\rho$ is dough density. To ensure that the dough covered the whole surface of the transducer, a value of $R$ (2.7 cm) was selected that was larger than transducer radius (2.2 cm). For the high frequency measurements, sample thickness was thin (<1 mm), and so subsample size was chosen by experience with the aim of attaining good transducer surface coverage. The circumference of both holders was sealed with tape to prevent moisture loss during ultrasonic measurements.

### 2.3. Analysis of ultrasonic data

#### 2.3.1. Analysis in the time domain

The low (40 kHz) frequency transducers had a narrow bandwidth, and it was assumed that dispersion of ultrasound in the dough would not occur over this narrow frequency range. Plots of the transit time of the first oscillation minimum and the amplitude of the first oscillation maximum as a function of sample thickness permitted the effects of impedance mismatches to be eliminated so that ultrasonic velocity and attenuation could be accurately determined [12].

Where only one subsample thickness was used, or where time evolution observations of a single sample were desired, a reference signal was used in conjunction with sample measurements for ultrasonic velocity and attenuation determination. The reference signal was measured with the two transducers in direct contact (*i.e.*, in the absence of the sample), or with a material
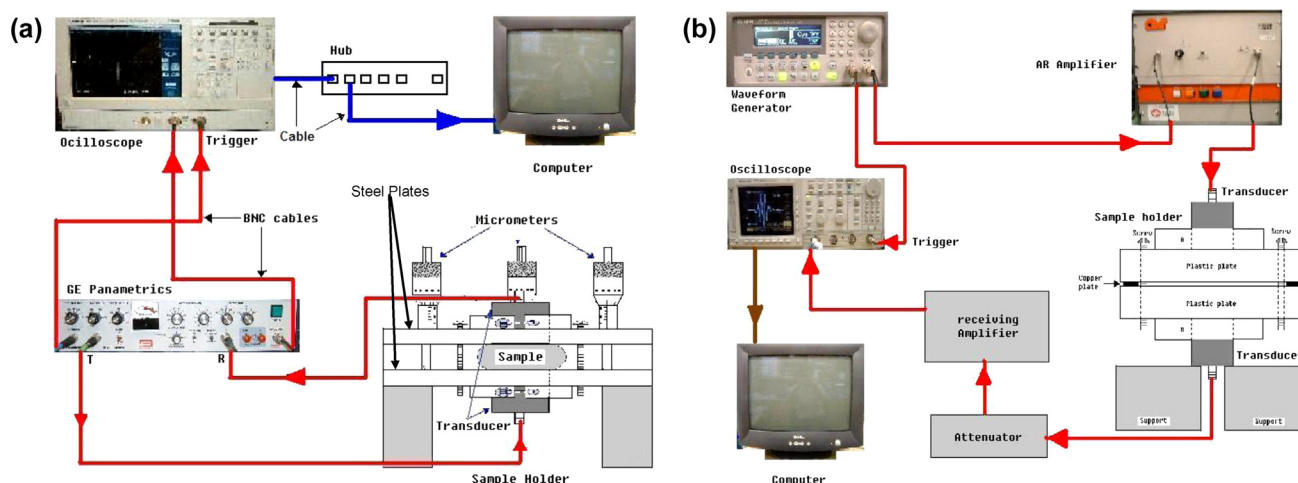
**Fig. 1.** Experimental set-ups for ultrasonic measurements at low (a) and high (b) frequencies, with the contact measurement holder being used for low frequencies and the acrylic plate delay measurement holder for high frequencies.

of well-known acoustic properties inserted between transducers. However, because impedance mismatches can reduce the transmitted signal amplitude as well as induce a phase shift that confounds velocity determination, a correction was required. Details of the impedance effect and calculation of the correction are discussed below.

### 2.3.2. Analysis in the frequency domain

To analyze the ultrasonic data in the frequency regime, a Fast Fourier Transform (FFT) method was used [50]. The FFT provides the frequency dependence of amplitude and phase from measurements of a subsample of given thickness. From the amplitude information, the attenuation coefficient can be acquired, and from phase information, the phase velocity can be determined [50].

### 2.3.3. Impedance correction in ultrasound measurements

When a sound wave travels across the boundary separating two materials, part of its wave energy is reflected from the boundary due to the different physical properties of the two materials [51,52]. During this process, both the amplitude and the phase may be changed. Three kinds of reference signal were used in order that the phase and amplitude were corrected for the effects of impedance mismatch, so that accurate velocity and attenuation coefficient measurements could be made.

The reference signals were a reference acquired when transducers were in direct contact, a reference through water, and a plastic layer reference. Specific impedance corrections differed for each reference type, the type of dough (vacuum or air mixed), and the transducer frequency. In all cases, the phase velocity and attenuation could be accurately determined by fixed-point iteration. Details of the methods used are too lengthy to include here, but are described fully by Fan [53].

## 3. Results and discussion

### 3.1. Mechanical spectrum of dough

The velocity and attenuation coefficient of dough over a wide frequency range are shown in Fig. 2 and in Fig. 3 for dough mixed at atmospheric pressure. The former shows the effect of changes in ultrasonic parameters with time after mixing, while the latter is for the same post-mixing time, but compares dough subsamples analyzed directly (2 min) after and 20 min after compressing subsamples between the transducers. The latter figure allows the

effect of time for dough relaxation in the experimental set-up to be observed. A time of 20 min was chosen since we expected substantial relaxation effects in dough to have occurred during this 20 min interval, based on results from spectroscopy [54,55], and from mechanical tests, where a time of 30 min is often cited
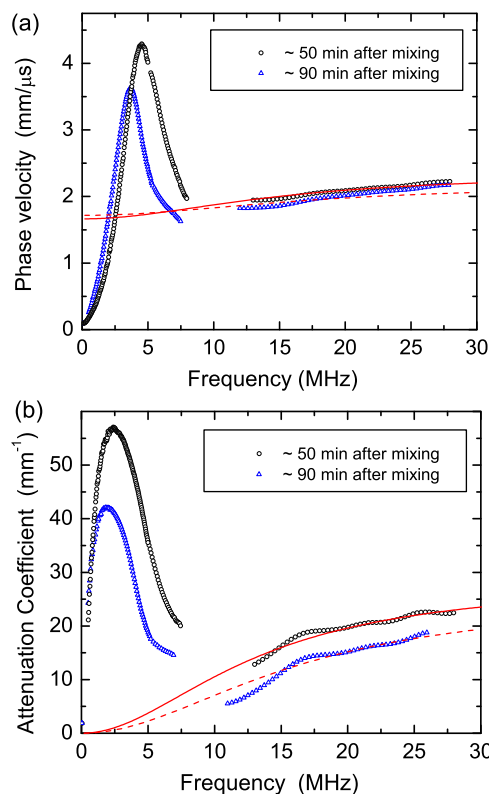


**Fig. 2.** Phase velocity (a) and attenuation coefficient (b) as a function of frequency for dough mixed at atmospheric pressure. Symbols represent experimental data measured with transducers of different central frequencies at different times after mixing ranging from 43 to 55 min (black circles) and 86 to 94 min (blue triangles). The solid and dashed red curves are fits of the relaxation model to the velocity and attenuation of the viscoelastic dough matrix that is measured at high frequencies (>10 MHz); the time after mixing for these high frequency data is 55 and 94 min (circles/solid curve and triangles/dashed curve, respectively). (For interpretation of the references to color in this figure legend, the reader is referred to the web version of the article.)
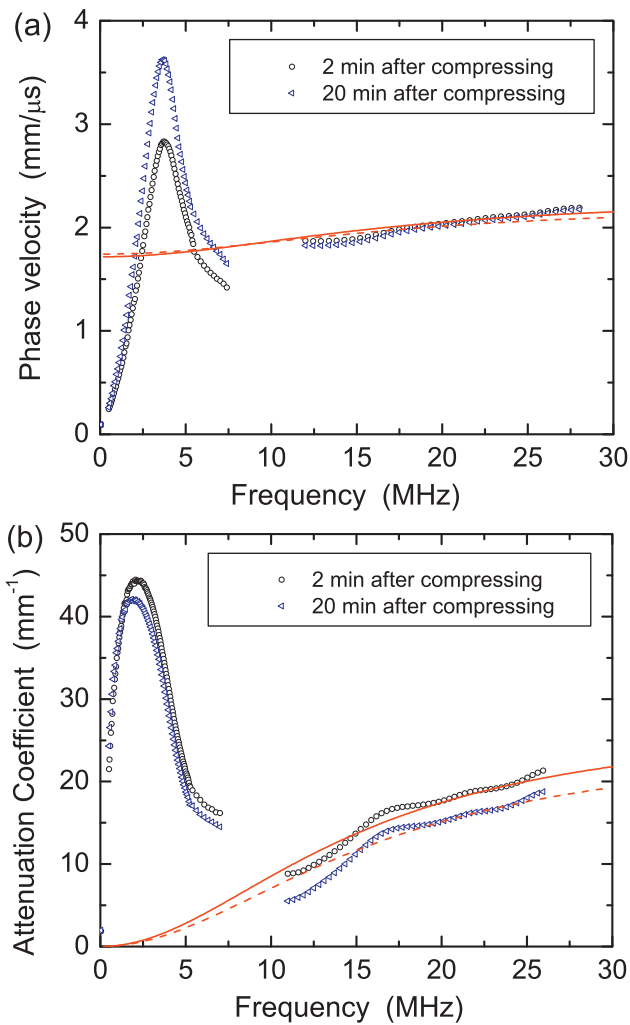
**Fig. 3.** Phase velocity (a) and attenuation coefficient (b) as a function of frequency for dough mixed at atmospheric pressure. Symbols represent data measured with transducers of different central frequencies at two different times after the dough samples were compressed in the transducer holders: 2 min after compressing (black circles) and 20 min after compressing (blue triangles). The time after mixing at the start of the measurements was approximately 70 min. The solid and dashed red curves are fits of the relaxation model to the high frequency (>10 MHz) velocity and attenuation for these two times after compressing. (For interpretation of the references to color in this figure legend, the reader is referred to the web version of the article.)

**Fig. 4.** Phase velocity (a) and attenuation coefficient (b) as a function of frequency for vacuum mixed dough. Symbols represent experimental data measured with transducers of different central frequencies at 2 min (green triangles) and 20 min (blue squares) after compressing. The time after mixing at the start of the measurements was approximately 70 min. The solid red curves are fits of the relaxation model to the high frequency (>10 MHz) velocity and attenuation. (For interpretation of the references to color in this figure legend, the reader is referred to the web version of the article.)

as sufficient time to dissipate stresses imposed during sample preparation [56,57].

The mechanical spectra at two different relaxation times after sample compression are shown in Fig. 4 for dough mixed under vacuum. As can be seen, no differences in phase velocity or attenuation coefficient were observed with relaxation time. Differences in spectra due to post-mixing time were also not evident [53].

It is worth drawing attention to the large difference in both the velocity and attenuation coefficient between the two types of dough, e.g., the velocity scale in Fig. 4 is magnified approximately 25 times relative to that of Fig. 2. For the dough that has been mixed at atmospheric pressure, the large peak in attenuation coefficient and the marked change in velocity for frequencies between 1 and 5 MHz arises from a broad resonance band associated with the polydisperse distribution of bubbles in the dough [22]; its analysis and interpretation has been covered elsewhere [48,58]. In this paper, an interpretation of the behavior at frequencies higher than the bubble resonance region is conducted, since it is at these higher frequencies that dough matrix properties can be accessed most directly
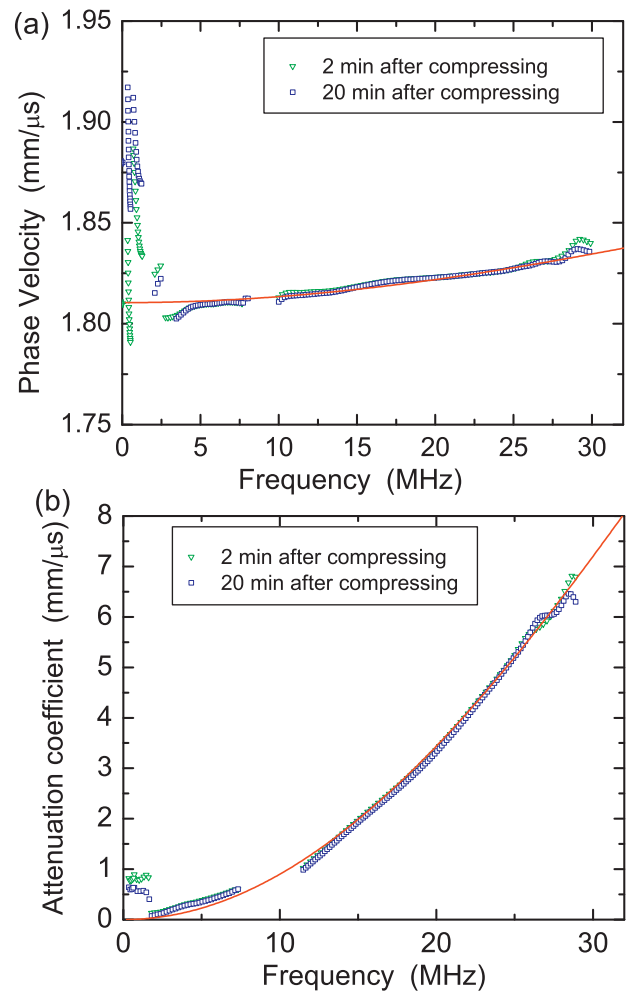
[43,48,58–61]. From a comparison of the two types of dough at these higher frequencies, the effect of internal interfacial area on the properties of the dough matrix can be ascertained.

### 3.2. Mechanical model for dough at frequencies far above bubble resonance

The model used to characterize the mechanical properties of the dough matrix is a classical ultrasonic relaxation model that describes how the frequency dependence of velocity and attenuation is influenced by molecular relaxations [59,61].

For longitudinal waves, the phase velocity, $v$, and the attenuation coefficient, $\alpha$, are related to the complex longitudinal modulus, $M^*$ ($M^* = M' + iM''$), of the dough as:

$$v = \sqrt{\frac{2}{\rho}\left(\frac{M'^2 + M''^2}{M' + \sqrt{M'^2 + M''^2}}\right)} \qquad (2)$$

$$\alpha = \omega \sqrt{2\rho \left( \frac{\sqrt{M'^2 + M''^2} - M'}{M'^2 + M''^2} \right)} \qquad (3)$$

where $\rho$ is dough density, $\omega$ is the angular frequency and $M'$ and $M''$ are the real and imaginary parts of the complex longitudinal modulus. The longitudinal modulus, $M^*$, that is measured with longitudinally polarized pulses is a function of both the complex bulk modulus, $K^*$, and the complex shear modulus, $G^*$ of the dough:

$$M^* = K^* + \frac{4}{3}G^* \qquad (4)$$

When a pressure pulse propagates in a viscoelastic medium, its mechanical response usually involves both volume and shear relaxations, with corresponding relaxation times of $\tau_v$ and $\tau_s$, respectively. Then, for the case where the static shear modulus is zero, i.e., treating the dough as a viscoelastic liquid [45,46], the complex moduli are related to the relaxation times as:

$$K^* = K_0 + \frac{K_r \omega^2 \tau_v^2}{1 + \omega^2 \tau_v^2} + i \frac{K_r \omega \tau_v}{1 + \omega^2 \tau_v^2} \qquad (5)$$

$$G^* = \frac{G_\infty \omega^2 \tau_s^2}{1 + \omega^2 \tau_s^2} + i \omega \frac{G_\infty \tau_s}{1 + \omega^2 \tau_s^2} \qquad (6)$$

where $K_0$ is the static bulk modulus, $K_r$ is the relaxational modulus, defined as $K_\infty - K_0$ (with $K_\infty$ being the high-frequency limit of the bulk modulus), $\tau_v$ is the relaxation time at constant volume, $\tau_s$ is the shear relaxation time, and $G_\infty$ is the high-frequency shear modulus. Predictions for the frequency dependence of the phase velocity and the attenuation coefficient in terms of these relaxation times and moduli can then be calculated by substituting Eqs. (4), (5) and (6) into (2) and (3). When $M'' \ll M'$, the expressions for $v$ and $\alpha$ simplify to:

$$v = \sqrt{\frac{K_0 + (K_r \omega^2 \tau_v^2/(1 + \omega^2 \tau_v^2)) + (4/3)(G_\infty \omega^2 \tau_s^2/(1 + \omega^2 \tau_s^2))}{\rho}} \qquad (7)$$

$$\alpha = \frac{\omega^2}{\rho v^3} \left( \frac{K_r \tau_v}{1 + \omega^2 \tau_v^2} + \left(\frac{4}{3}\right) \frac{G_\infty \tau_s}{1 + \omega^2 \tau_s^2} \right) \qquad (8)$$

These expressions describe the effect on velocity and attenuation of the absorption of acoustic energy by biopolymers in the dough when this process requires some finite amount of time for energy exchange due to volumetric and shear relaxations. As a result, the velocity and the attenuation coefficient vary with frequency, with the magnitude of the changes in velocity and attenuation being determined by the moduli, and the frequency range over which these changes occur being determined by the relaxation times. Since the bulk modulus is orders of magnitude larger than the shear modulus in dough [46,47] and other soft solids [62,63], the magnitude of the shear relaxation was believed to be small enough that there would be an insignificant effect on the longitudinal phase velocity and attenuation coefficient. Thus, Eqs. (7) and (8), and also the exact expressions obtained from (2) and (3) without the approximation that $M'' \ll M'$, were simplified before fitting the theory to the experimental data by setting the shear modulus, $G_\infty$, to zero.

### 3.3. Comparison of experimental and mechanical model predictions

Ultrasonic data for the doughs that had been mixed in air were compared with the predictions of the model for different post-mixing times as well as different post-compression times. Two post-mixing times are reported here to illustrate this effect on the mechanical response of the dough. Both data sets were selected

**Table 1**
Model fitting parameters at two different post-mixing times for dough mixed at atmospheric pressure (volume fraction of gas in the dough = 0.11).

| Post mixing time/min | $K_0$/GPa | $K_r$/GPa | $\tau_v$/ns |
|---|---|---|---|
| 55 | $3.1 \pm 0.2$ | $3.05 \pm 0.1$ | $7.5 \pm 1$ |
| 94 | $3.3 \pm 0.2$ | $2.05 \pm 0.2$ | $7 \pm 1$ |

Uncertainties correspond to one standard deviation of the best fit parameters.

**Table 2**
Model fitting parameters at two different relaxation times after mounting the dough in the transducer assembly for dough that had been mixed at atmospheric pressure (volume fraction of gas in the dough = 0.11).

| Relaxation time/min | $K_0$/GPa | $K_r$/GPa | $\tau_v$/ns |
|---|---|---|---|
| 2 | $3.3 \pm 0.2$ | $2.6 \pm 0.2$ | $7.0 \pm 1.5$ |
| 20 | $3.3 \pm 0.2$ | $2.05 \pm 0.2$ | $7.0 \pm 1.5$ |

Uncertainties correspond to one standard deviation of the best fit parameters.

from ultrasonic measurements performed 20 min after compressing so that stress relaxation effects associated with mounting the dough in the transducer assembly should be identical. The fitting of this model to the high frequency ultrasonic results for dough measured both 55 and 94 min after mixing is shown in Fig. 2 by the solid and dashed curves, respectively, with the best-fit values of parameters found from the model presented in Table 1, using the measured dough density of 1120 kg/m³. It is important to emphasize that in fitting Eqs. (7) and (8) to the data, predictions for the phase velocity and attenuation coefficient must use common values for the moduli and relaxation times, so that attaining the good fits that are evident in Fig. 2 is constrained by this requirement.

From Table 1, it is apparent that the value of the relaxation modulus decreases significantly as post-mixing time increases, reflecting the drop in both attenuation coefficient and velocity that are observed at the longer time (Fig. 2). The volumetric relaxation time associated with this material, which stiffens with increasing frequency, is approximately 7 ns, regardless of time after mixing.

Because of stress relaxation effects in dough [54–57], we also investigated air-mixed samples almost immediately after compression (2 min) and 20 min after compression; the corresponding post-mixing times are 76 and 94 min (Fig. 3). Effects of changes in properties due to relaxation in the sample holder are superposed on effects due to post-mixing time. The results of modeling of these high frequency data are shown in Table 2. Again, in both cases, a value for the relaxation time at constant volume is obtained that is approximately 7 ns.

For the doughs mixed under vacuum, we did not observe any post-mixing time changes in velocity and attenuation coefficient, and, as might be expected from observation of Fig. 4, there was no difference between the model fits for data from dough tested 2 min after compression and dough tested 20 min after compression. The results of fitting the model to the experimental data are shown in Fig. 4 by the solid curves and the corresponding fitting parameters are listed in Table 3, using the experimentally determined value for the density of vacuum-mixed dough (1260 kg/m³).

Although the mechanical properties of vacuum-mixed dough do not change with time in this high frequency range, the vacuum dough stiffens as frequency increases just as the dough mixed at atmospheric pressure does. The value calculated for $K_\infty$

**Table 3**
Model fitting parameters for dough mixed under vacuum.

| $K_0$/GPa | $K_r$/GPa | $\tau_v$/ns |
|---|---|---|
| $4.13 \pm 0.01$ | $1.02 \pm 0.15$ | $1.7 \pm 0.3$ |

Uncertainties correspond to one standard deviation of the best fit parameters.

$(K_\infty = K_0 + K_r \approx 5\,\text{GPa})$ is very similar to that of the dough mixed at atmospheric pressure (5–6 GPa). However, the relaxation time at constant volume for the vacuum-mixed dough is substantially lower (by a factor of approximately ¼), with a best-fit value of 1.7 ns.

### 3.4. Structural and/or molecular basis for the high frequency ultrasonic relaxations

To relate the high frequency ultrasonic relaxations to a specific molecular process in the dough matrix, we need to find a mechanism that incorporates the following experimental outcomes. There is essentially no difference in the value of $K_\infty$ for both types of dough at long times after the dough subsamples have been compressed, whereas the value of $K_0$ is larger for the dough with very little internal interfacial area, i.e., the vacuum mixed dough (4 vs 3 GPa). This means that the zero frequency bulk modulus of the dough mixed in air is smaller than that of a vacuum-mixed dough, a result consistent with the latter material's lower moisture content. Secondly, the change in mechanical properties as a function of frequency can be modeled with a single relaxation mechanism that is relatively long in doughs with substantial internal interfacial area (7 ns vs ~2 ns). Before identifying a plausible mechanism that accounts for these observations, we discuss some putative molecular relaxation phenomena that can be shown to be not responsible.

Firstly, differences between the two types of dough are not due to a mechanical relaxation associated with configurational rearrangements of free water molecules within the dough. These relaxations occur over picosecond timeframes [64–66] and so would not influence the behavior seen over the frequency range of the current ultrasonic experiments. However, since water molecules associated with proteins can undergo rotation at much slower timescales [64,66], the role of "bound" water in the mechanical relaxation cannot be ruled out.

Secondly, it is not a molecular relaxation time associated with rotation or tumbling of the protein molecules in the aqueous environment in which they reside. The classical equation relating rotational correlation times ($\tau_R$) to molecular volume ($V$) in a solvent of given viscosity ($\eta$) is given by [66,67]:

$$\tau_R = \frac{\eta V}{k_B T}, \tag{9}$$

in which $k_B$ is Boltzmann's constant and $T$ is absolute temperature. Given the large molecular volume associated with gluten proteins [55,68,69], we cannot attribute a mechanical relaxation that takes less than 10 ns to tumbling of the glutenin or gliadin molecules that make up the gluten proteins within the dough matrix. For example, Yeboah et al. [67] found from time-resolved fluorescence analyses that the rotational correlation time of γ-gliadins in 70% ethanol was of the order of 50 ns. Since the γ-gliadins are one of the smallest storage proteins found in the dough matrix [70], rotations of the protein molecules themselves can be ruled out as the basis for the observed ultrasonic relaxations.

Thirdly, the time scale is too short for full-scale folding of the proteins into a new conformation as a result of the mechanical disturbance by the ultrasonic pulses. For large proteins, such conformational changes take place over timescales of milliseconds to seconds [71,72]. Even longer timescales have been associated with conformational changes of proteins residing at interfaces [73,74].

Therefore, we propose that intermediate length-scale folding motions in the gluten proteins or the protein-water complex must be responsible for the 2–7 ns timescale relaxations that are observed with our ultrasonic spectroscopy measurements. One likely mechanism is ultrasonic stress-induced changes in the secondary structure of gluten proteins. A number of electromagnetic spectroscopic analyses have confirmed the occurrence of
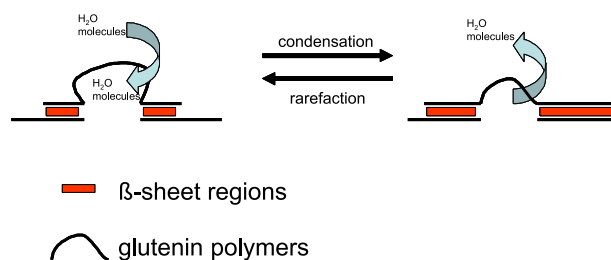


**Fig. 5.** Conformational rearrangements in glutenin induced by a sinusoidally varying ultrasonic pulse.

intermediate length-scale folding motions in gluten proteins [67,75–77]. In particular, the interconversion from $P_{II}$, disordered or $\beta$-turn structures to the $\beta$-sheet structure is a means of storing the elastic energy [55,78] that is put into the system by the ultrasonic pulses. The timescale for such conformational rearrangements is of the order of nanoseconds [39,67], and so matches the relaxation times of these studies. Nevertheless, if we are to explain the ultrasonic results as arising from secondary structural rearrangements in the gluten proteins, an explanation for why this conformational rearrangement occurs four times faster in doughs mixed under vacuum compared to air-mixed doughs is needed.

In proposing a potential mechanism for the relaxation time difference, we take the viewpoint of Belton and colleagues that the loop and train model is an apt description of the structure of wheat glutenins [79]. We also suggest that ultrasonic strain energy at lower frequencies induces the disordered (hydrophilic) to $\beta$-sheet conformation transition in glutenin described above, and thus elastic energy is stored in the dough matrix. The creation of a greater amount of $\beta$-sheet structure in the glutenin leads to loss of water from the loop regions of the glutenin polymers [76,77] as schematically illustrated in Fig. 5.

In the condensation phase, water molecules that are hydrogen bonded to the many glutamine side-chains on the polymers are squeezed out of the loops so that strain energy can be stored in the $\beta$-sheet regions (trains) where glutamine hydrogen bonds to glutamine on an adjacent chain, and this hydrogen bonded structure is then reinforced by hydrophobic bonds [76]. At low frequencies, the efflux of water molecules from the loops during the condensation phase acts in phase with the ultrasound and so attenuation losses arising from this process are negligible. In this low frequency regime, the dough with more train regions will be less compressible than its counterpart that possesses more loop regions. The less compressible dough will be the dough with less moisture [77], i.e., the dough that has been mixed under vacuum.

At very high frequencies (likely >100 MHz), the structural transition induced by ultrasonic condensation cannot take place since there is insufficient time for water movement from the loops and for the creation of a greater amount of $\beta$-sheet regions. In this case, there will be no difference in the $K_\infty$ values for the two types of doughs, a result that is predicted by the model fits to the data, i.e., at very high frequencies the bulk modulus of the dough is independent of its water content.

In the intermediate timescales the loop to train transition does occur, but there is a phase lag between the ultrasonic wave and the movement of water back into the loops during the rarefactions. As a result, a greater loss of acoustic energy occurs, with the rapid rise in the attenuation centered at a frequency that is close to the reciprocal of the relaxation time for water movement into and out of the loops. To explain our results, it is therefore necessary to suggest molecular structures in the glutenin polymers that would cause the relaxation time to be four times slower in the dough mixed in air compared to the dough mixed under vacuum.

We propose that the slower relaxation time for the air-mixed doughs is due to the presence of bubbles. The loop-to-train transition is harder to induce in the air-mixed doughs because the polymers that undergo this transition are tethered by the attachment of surface-active regions of their molecules to the bubbles associated with the large internal interfacial area. Wheat gluten proteins are surface-active polymers, and would be expected to lower their overall free energy state by adopting a conformation where hydrophobic regions of the polymer reside at the air-aqueous interface [32] or by their interaction with polymers that are highly surface-active [80]. For example, when ovalbumin adsorbs at an air-aqueous interface, protein movement at the nanosecond timescale becomes more restricted [39]. If this also occurs for the surface active storage proteins in dough, then the considerable amount of interfacial area in doughs [26] would be expected to retard the conversion of loops to trains and so increase the relaxation time in doughs mixed under air that have this large interfacial area.

## 4. Conclusions

A very broad frequency characterization of the mechanical spectra of dough by longitudinally polarized ultrasound revealed pronounced differences in phase velocity and attenuation coefficient for dough mixed in air compared to dough mixed under vacuum, a result attributable to the presence of bubbles in air-mixed dough. In the high frequency regime, where biopolymer effects are evident, a single volumetric relaxation mechanism was seen. The time taken for this to occur in air-mixed dough (7 ns) was significantly longer than in dough devoid of bubbles. This was attributed to tethering of amphiphilic portions of gluten molecules to the large interfacial area in air-mixed doughs.

## Acknowledgment

## References

[1] N. Wellner, J.T. Marsh, A.W.J. Savage, N.G. Halford, P.R. Shewry, E.N.C. Mills, P.S. Belton, Biomacromolecules 7 (2006) 1096.
[2] B. Lagrain, B. Goderis, K. Brijs, J.A. Delcour, Biomacromolecules 11 (2010) 533.
[3] P.R. Shewry, N.G. Halford, P.S. Belton, A.S. Tatham, Philos. Trans. R. Soc. London Ser. B 357 (2002) 133.
[4] V. Ducel, P. Saulnier, J. Richard, F. Boury, Colloids Surf. B: Biointerfaces 41 (2005) 95.
[5] N. Gontard, S. Guilbert, J.L. Cuq, J. Food Sci. 57 (1992) 190.
[6] J.A. Bietz, G.L. Lookhart, Cereal Foods World 41 (1996) 376.
[7] L. Liao, Y. Luo, M. Zhao, Q. Wang, Colloids Surf. B: Biointerfaces 92 (2012) 305.
[8] N. Chamberlain, T.H. Collins, Baker's Digest 53 (1) (1979) 18.
[9] G.M. Campbell, C.D. Rielly, P.J. Fryer, P.A. Sadd, Cereal Foods World 43 (1998) 163.
[10] M.B. Whitworth, J.M. Alava, in: G.M. Campbell, C. Webb, S.S. Pandiella, K. Niranjan (Eds.), Bubbles in Food, Eagan Press, St. Paul, MN, 1999, p. 221.
[11] K.L. Mehta, M.G. Scanlon, H.D. Sapirstein, J.H. Page, J. Food Sci. 74 (2009) E455.
[12] H.M. Elmehdi, J.H. Page, M.G. Scanlon, Cereal Chem. 81 (2004) 504.
[13] J.C. Baker, M.D. Mize, Cereal Chem. 23 (1946) 39.
[14] G.M. Campbell, C.D. Rielly, P.J. Fryer, P.A. Sadd, Cereal Chem. 70 (1993) 517.
[15] B.J. Dobraszczyk, G.M. Campbell, Z. Gan, in: D.A.V. Dendy, B.J. Dobraszczyk (Eds.), Cereals and Cereal Products: Chemistry and Technology, Aspen Publishers, Gaithersburg, MD, 2001, p. 182.
[16] G.M. Campbell, P.J. Martin, in: S.P. Cauvain (Ed.), Breadmaking: Improving Quality, 2nd ed., Woodhead, Cambridge, UK, 2012, p. 299.
[17] P. Babin, G. Della Valle, R. Dendievel, N. Lassoued, L. Salvo, J. Mater. Sci. 40 (2005) 5867.
[18] P. Babin, G. Della Valle, H. Chiron, P. Cloetens, J. Hoszowska, P. Pernot, A.L. Réguerre, L. Salvo, R. Dendievel, in: G.M. Campbell, M.G. Scanlon, L.S. Pyle (Eds.), Bubbles in Food, 2: Novelty, Health and Luxury, AACC Press, St. Paul, MN, 2008, p. 265.
[19] S. Guessasma, P. Babin, G. Della Valle, R. Dendievel, Int. J. Solids Struct. 45 (2008) 2881.
[20] N.L. Chin, P.J. Martin, G.M. Campbell, J. Sci. Food Agric. 85 (2005) 2203.
[21] C. Wang, S. Dai, R.I. Tanner, Korea-Australia Rheol. J. 18 (2006) 127.
[22] M.G. Scanlon, H.M. Elmehdi, V. Leroy, J.H. Page, in: G.M. Campbell, M.G. Scanlon, L.S. Pyle (Eds.), Bubbles in Food, 2: Novelty, Health and Luxury, AACC Press, St. Paul, MN, 2008, p. 217.
[23] G.M. Campbell, C.D. Rielly, P.J. Fryer, P.A. Sadd, Trans. Inst. Chem. Eng., C 69 (1991) 67.
[24] Y. Shimiya, K. Nakamura, J. Texture Stud. 28 (1997) 273.
[25] G.G. Bellido, M.G. Scanlon, J.H. Page, B. Hallgrimsson, Food Res. Int. 39 (2006) 1058.
[26] T. Carlson, L. Bohlin, Cereal Chem. 55 (1978) 539.
[27] R.J. Fajardo, T.M. Ryan, J. Kappelman, Am. J. Phys. Anthropol. 118 (2002) 1.
[28] X.S. Liu, X.H. Zhang, K.K. Sekhon, M.F. Adams, D.J. McMahon, J.P. Bilezikian, E. Shane, X.E. Guo, J. Bone Miner. Res. 25 (2010) 746.
[29] J. Zeschky, T. Hofner, C. Arnold, R. Weißmann, D. Bahloul-Hourlier, M. Scheffler, P. Greil, Acta Mater. 53 (2005) 927.
[30] J. Ornebro, T. Nylander, A.C. Eliasson, J. Cereal Sci. 31 (2000) 195.
[31] E.N.C. Mills, P.J. Wilde, L.J. Salt, P. Skeggs, Food Bioprod. Process. 81 (2003) 189.
[32] P. Wilde, in: S.P. Cauvain (Ed.), Breadmaking: Improving Quality, 2nd ed., Woodhead, Cambridge, UK, 2012, p. 370.
[33] Z. Z. Gan, P.R. Ellis, J.D. Schofield, J. Cereal Sci. 21 (1995) 215.
[34] B.S. Sroan, S.R. Bean, F. MacRitchie, J. Cereal Sci. 49 (2009) 32.
[35] J.R. Clarkson, Z.F. Cui, R.C. Darton, J. Colloid Interface Sci. 215 (1999) 333.
[36] M.A. Bos, B. Dunnewind, T. van Vliet, Colloids Surf. B: Biointerfaces 31 (2003) 95.
[37] J.P. Davis, D. Doucet, E.A. Foegeding, J. Colloid Interface Sci. 288 (2005) 412.
[38] H. Zhu, S. Damodaran, J. Agric. Food Chem. 42 (1994) 846.
[39] E.V. Kudryashova, M.B.J. Meinders, A.J.W.G. Visser, A. van Hoek, H.H.J. de Jongh, Eur. Biophys. J. 32 (2003) 553.
[40] A.R. Mackie, A.P. Gunning, P.J. Wilde, V.J. Morris, J. Colloid Interface Sci. 210 (1999) 157.
[41] E.W. Blanch, D.D. Kasarda, L. Hecht, K. Nielsen, L.D. Barron, Biochemistry 42 (2003) 5665.
[42] C. Le Floch-Fouere, S. Pezennec, V. Lechevalier, S. Beaufils, B. Desbat, M. Pezolet, A. Renault, Food Hydrocolloids 23 (2009) 352.
[43] J.D. Ferry, Viscoelastic Properties of Polymers, John Wiley and Sons, New York, NY, 1961.
[44] R.I. Tanner, F. Qi, S.-C. Dai, J. Non-Newtonian Fluid Mech. 148 (2008) 33.
[45] T.S.K. Ng, G.H. McKinley, J. Rheol. 52 (2008) 417.
[46] V. Leroy, K.M. Pitura, M.G. Scanlon, J.H. Page, J. Non-Newtonian Fluid Mech. 165 (2010) 475.
[47] C. Létang, M. Piau, C. Verdier, L. Lefebvre, Ultrasonics 39 (2001) 133.
[48] V. Leroy, Y. Fan, A.L. Strybulevych, G.G. Bellido, J.H. Page, M.G. Scanlon, in: G.M. Campbell, M.G. Scanlon, L.S. Pyle (Eds.), Bubbles in Food, 2: Novelty, Health and Luxury, AACC Press, St. Paul, MN, 2008, p. 51.
[49] I. Hlynka, J.A. Anderson, Cereal Chem. 32 (1955) 83.
[50] L.A.E.B. Cobus, K.A. Ross, M.G. Scanlon, J.H. Page, J. Agric. Food Chem. 55 (2007) 8889.
[51] I. Malecki, Physical Foundations of Technical Acoustics (I. Bellert, Translator), Pergamon Press, Oxford, 1969.
[52] H. Kuttruff, Ultrasonics Fundamentals and Applications, Elsevier Applied Science, London, 1991.
[53] Y. Fan, Using ultrasound to investigate relaxation and resonance phenomena in wheat flour dough, MSc Thesis, University of Manitoba, Winnipeg, MB, 2006.
[54] P.T. Callaghan, A.M. Gil, Rheol. Acta 38 (1999) 528.
[55] N. Wellner, E.N.C. Mills, G. Brownsey, R.H. Wilson, N. Brown, J. Freeman, N.G. Halford, P.R. Shewry, P.S. Belton, Biomacromolecules 6 (2005) 255.
[56] A.M. Janssen, T. van Vliet, J.M. Vereijken, J. Cereal Sci. 23 (1996) 43.
[57] P. Masi, S. Cavella, M. Sepe, Cereal Chem. 75 (1998) 428.
[58] V. Leroy, A. Strybulevych, J.H. Page, M.G. Scanlon, J. Acoust. Soc. Am. 123 (2008) 1931.
[59] T.A. Litovitz, C.M. Davis, Physical Acoustics Volume II, Part A, Academic Press, London, 1965, pp. 281.
[60] M.J.W. Povey, Ultrasonic Techniques for Fluid Characterization, Academic Press, San Diego, 1997.
[61] C. Verdier, P.-Y. Longin, M. Piau, Rheol. Acta 37 (1998) 234.
[62] D.J. McClements, Crit. Rev. Food Sci. Nutr. 37 (1997) 1.
[63] C. Verdier, M. Piau, J. Acoust. Soc. Am. 101 (1997) 1868.
[64] B. Bagchi, Chem. Rev. 105 (2005) 3197.
[65] G. Caliskan, A. Kisliuk, A.M. Tsai, C.L. Soles, A.P. Sokolov, J. Chem. Phys. 118 (2003) 4230.
[66] B. Halle, Philos. Trans. R. Soc. London Ser. B 359 (2004) 1207.
[67] N.A. Yeboah, R.B. Ferredman, Y. Popineau, P.R. Shewry, A.S. Tatham, J. Cereal Sci. 19 (1994) 141.
[68] A.H. Bloksma, Cereal Foods World 35 (1990) 228.
[69] N. Phan-Thien, M. Newberry, R.I. Tanner, J. Non-Newtonian Fluid Mech. 92 (2000) 67.
[70] J.-C. Autran, in: J.E. Kruger, J.A. Bietz (Eds.), High-Performance Liquid Chromatography of Cereal and Legume Proteins, AACC Press, St Paul, MN, 1994, p. 326.
[71] W. Guo, J.-E. Shea, R.S. Berry, Ann. N.Y. Acad. Sci. 1066 (2005) 34.
[72] A.N. Naganathan, U. Doshi, A. Fung, M. Sadqi, V. Muñoz, Biochemistry 45 (2006) 8466.
[73] A.H. Martin, M.B.J. Meinders, M.A. Bos, M.A. Cohen Stuart, T. van Vliet, Langmuir 19 (2003) 2922.
[74] Y.F. Yano, J. Phys.: Condens. Matter 24 (2012) 503101.

[75] L. Calucci, C.P. Filipczynskiino, A. Capocchi, L. Galleschi, S. Ghiringhelli, F. Saviozzi, M. Zandomeneghi, J. Agric. Food Chem. 49 (2001) 359.

[76] E. Alberti, S.M. Gilbert, A.S. Tatham, P.R. Shewry, A.M. Gil, Biopolymers (Biospectroscopy) 67 (2002) 487.

[77] D.M.R. Georget, P.S. Belton, Biomacromolecules 7 (2006) 469.

[78] Z. Shi, K. Chen, Z. Liu, N.R. Kallenbach, Chem. Rev. 106 (2006) 1877.

[79] P.S. Belton, J. Cereal Sci. 29 (1999) 103.

[80] S.J. Haward, P.R. Shewry, M.J. Miles, T.J. Mcmaster, Biopolymers 93 (2010) 74.